# Hybrid sequential deposition process for fully textured silicon/perovskite tandem solar cells

Florent Sahli,[a] Jérémie Werner,[a] Brett Kamino,[b] Matthias Bräuninger,[a] Chien-Jen Yang,[a] Peter Fiala,[a] Gizem Nogay,[a] Fan Fu,[a] Raphäel Monnard,[a] Arnaud Walter,[b] Soo-Jin Moon,[b] Esteban Rucavado,[a] Loris Barraud,[b] Bertrand Paviet-Salomon,[b] Christophe Allebé,[b] Laura Ding,[b] Juan Diaz,[b] Davide Sacchetto, [b] Gianluca Cattaneo, [b] Monica Morales-Masis,[a] Mathieu Boccard,[a] Matthieu Despeisse,[b] Sylvain Nicolay,[b] Quentin Jeangros,[a] Bjoern Niesen,[b] and Christophe Ballif[a,b]

[a] Ecole Polytechnique Fédérale de Lausanne (EPFL), Institute of Microengineering **(**IMT**)** Photovoltaics and Thin-Film Electronics Laboratory (PV-Lab), Rue de la Maladière 71b, 2002 Neuchâtel, Switzerland.

[b] CSEM, PV-Center, Jaquet-Droz 1, 2002 Neuchâtel, Switzerland.

***Abstract* — Tandem solar cells that feature a high bandgap perovskite on top of a lower bandgap silicon cell have the potential to reach efficiencies >30%. Here, we present a versatile hybrid deposition method that yields conformal perovskite cells directly on textured silicon bottom cells, a requisite to achieve highest photocurrents and hence efficiencies. Furthermore, this low temperature evaporation/spin-coating method produces high quality perovskite materials with different bandgaps, here varied in the range 1.5 eV to 1.8 eV. This flexibility enables the fabrication of monolithic 2-terminal perovskite/textured Si tandems that feature high photocurrents of about 19.5 mA/cm$^2$.**

***Index Terms* — amorphous silicon, hybrid organic inorganic perovskites, monolithic, multijunction solar cells, silicon heterojunction solar cells.**

## I. Introduction

Crystalline silicon solar cells are approaching their theoretical Auger limit of 29.4% with a current record at 26.6% [1]. One promising approach to overcome this limit relies on reducing thermalization losses by stacking several absorbers of different bandgaps together in a multi-junction device. In that regard, perovskite solar cells have been identified as a promising top cell partner for crystalline silicon. This stems from the perovskite's potential low cost, its bandgap that can be tuned in the ideal range for tandems and its high power conversion efficiency [1]. Thanks to these advantages, perovskite/silicon tandem solar cells have an efficiency potential >30% at reasonable production costs [2]-[3]. Promising efficiencies have been demonstrated experimentally, both for monolithic (2-terminal, >22% [4]-[5]) and mechanically stacked (4-terminal) configurations (>25% [6]-[7]). To improve these values beyond 30%, the perovskite cell should i) have a bandgap ($E_g$) of ~1.7 eV [8] (currently ~1.6 eV for record devices), ii) exhibit an open circuit voltage as close as possible to this bandgap and iii) generate a high photocurrent matched to the one of the silicon bottom cell (in a monolithic 2-terminal configuration). This last point can be achieved by switching from a silicon bottom cell with a polished front side as in today's record devices to a fully textured one to maximize light trapping. Yet this prevents the use of conventional solution processing techniques to deposit the perovskite top cell. To tackle that issue, we present a co-evaporation/spin coating method that produces conformal $CsFAPb(I_{1-x}Br_x)_3$ perovskite-based cells, also on textured substrates. This composition can be tuned to reach $E_g$ suited for tandems and has been shown to yield efficient cells with long term stability [4][9]. The bandgap is varied here in the range 1.5-1.8 eV using various Cs-halide precursors, evaporation rates and organo-halide solutions. After extensive characterization of the optolectronic and microstructural properties of individual perovskite layers and single junction devices, perovskite/textured Si monolithic tandems with current densities of ~19.5 mA/cm$^2$ are demonstrated.

## II. Experimental methods

Planar perovskite solar cells are deposited in both *p-i-n* or *n-i-p* polarities on glass/ITO substrates (for single junctions) and in the *p-i-n* configuration on Si bottom cells for tandems. The latter polarity has been chosen to prevent parasitic absorption in the hole conducting spiro-OMeTAD layer, which has been identified as a major loss in perovskite/silicon tandems [10]. The bottom cells are rear emitter n-type silicon heterojunction solar cells, which feature intrinsic and doped hydrogenated amorphous silicon layers as carrier-selective contacts.

*p-i-n* perovskite cells feature either thermally evaporated spiro-TTB or sputtered $NiO_x$ as a hole contact. Absorbers of different compositions are grown using an hybrid sequential two-step method. It involves co-evaporating $PbI_2$ with a Cs-based halide (CsI, CsCl or CsBr) at different relative rates and then spin coating a formamidinium iodide and bromide mixture (FAI and FABr). An annealing step at 150°C for 30 min then crystallizes the perovskite. A layer stack of $C_{60}$ and TmPyPB is thermally evaporated to form the electron contact. For opaque cells, Ag is evaporated either over the entire cell. Alternatively, a stack of $SnO_2$ (by atomic

layer deposition) and indium zinc oxide (IZO, sputtered) and Ag fingers (evaporation) is used for semi-transparent cells. *N-i-p* cells involved a similar process but with a different hole contact, spiro-OMeTAD.
The optical and microstructural properties of perovskite layers and devices of different bandgaps were retrieved using UV–vis–NIR spectrophotometry, spectroscopic ellipsometry, Fourier transform photocurrent spectroscopy (FTPS), photothermal deflection spectroscopy (PDS), X-ray diffraction (XRD), scanning electron microscopy (SEM), transmission electron microscopy (TEM) and atomic force microscopy (AFM). Solar cells were characterized using current-voltage (two-lamp halogen and xenon class AAA WACOM sun simulator with an AM1.5g irradiance spectrum) and external quantum efficiency (EQE, custom-made set-up) measurements.

## III. Results and Discussion

Aborptance spectra of perovskite layers deposited on glass with different Cs-halide over $PbI_2$ evaporation rate ratios (% in the legend) and FAI over FABr concentrations (X:Y in the legend) are presented in Figure 1. Characterization also included ellipsometry, FTPS, PDS, XRD and AFM. The perovskite $E_g$ can be tuned between 1.5 and 1.8 eV. Increasing the Br over I ratio widen the bandgap. This can be achieved using solutions more concentrated in FABr. Similarly, the use of CsBr instead of CsI during co-evaporation yields a larger $E_g$. Interestingly, CsCl-based perovskites exhibit the highest $E_g$, indicating that Cl is a suitable precursor for tandem applications.

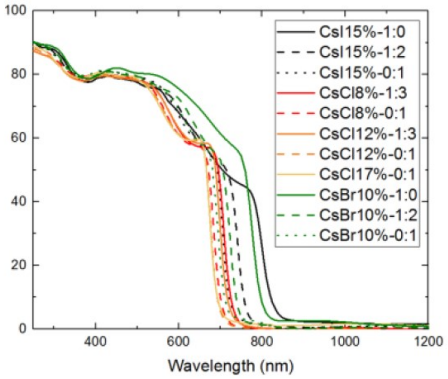


*Figure 1: Absorptance spectra of different perovskite films on glass. Perovskites were obtained using different cesium precursors and evaporate rates (%) and varying the FABr:FAI (X:Y) concentrations.*

Single junction devices with these perovskite compositions were fabricated in either *p-i-n* (opaque cells) or *n-i-p* (semi-transparent cells) configurations. Figure 2 shows a scanning TEM micrograph and the corresponding energy-dispersive X-ray (EDX) spectroscopy data of one of these devices: a 1.7 eV *p-i-n* CsI-based cell.

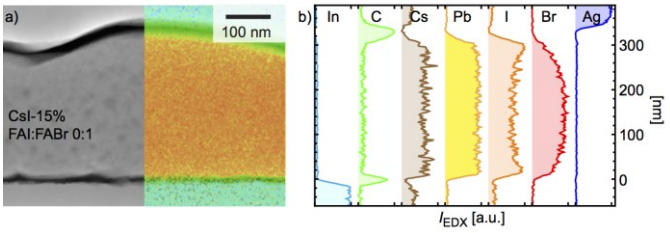


*Figure 2: a) Scanning TEM micrograph and corresponding EDX map of a perovskite cell produced by co-evaporating CsI and $PbI_2$ precursors, b) background-subtracted intensity profiles of the different elements present in the cell.*

The *J-V* characteristics of the different devices are investigated as a function $E_g$ in Figure 3. As expected, the open-circuit voltage ($V_{oc}$) increases with $E_g$. The voltage deficit is still quite far from optimal values and is mainly attributed to recombinations at interfaces between the perovskite layer and the charge extraction layers. In comparison, *p-i-n* cells exhibit a $V_{oc}$ that is 25-50 mV lower than *n-i-p* cells due to suboptimal interfaces. Interface engineering or alternative contact materials should help reducing this loss in $V_{oc}$. The gain in $V_{oc}$ with $E_g$ becomes less important >1.7 eV due to the segregation of I and Br as observed in Figure 2 and reported [11].
The short-circuit current density ($J_{sc}$) decreases with increasing $E_g$ as less photons are harvested by wider-bandgap perovskites. Most efficient devices are obtained with a $E_g$ of 1.6-1.65 eV. At higher $E_g$, the gain in $V_{oc}$ is not sufficient to compensate the loss in $J_{sc}$ and fill-factor.

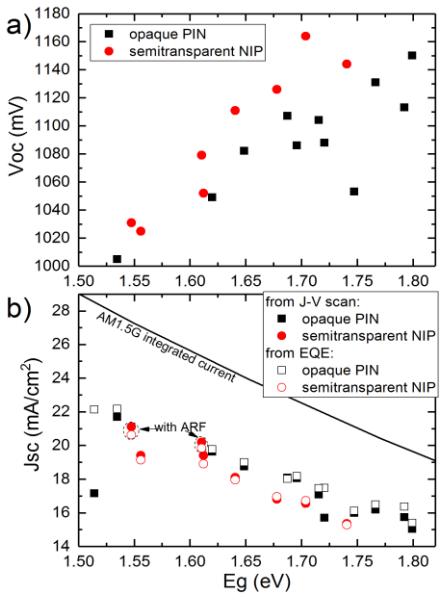


*Figure 3: a) $V_{oc}$ and b) $J_{sc}$ of perovskite solar cells as function of their optical bandgap.*

The main advantage of this deposition method is its ability to deposit conformal perovskite layers on rough substrates. This is of interest to manufacture tandem devices that feature commercially available textured silicon wafer. Figure 4a shows a cross section SEM image of a perovskite cell deposited directly on a textured silicon heterojunction. The perovskite and charge transport layers have a uniform thickness, covering conformally the summits, edges and valleys of the Si pyramids. With this architecture, light reflection at the front of the device is strongly mitigated, which enhances the current generated in both subcells. A 1.59 eV perovskite bottom cell is selected here to approach current-matching conditions: 19.5 mA/cm$^2$ in the perovskite and >20 mA/cm$^2$ in the silicon cell (Figure 4b). With such design, power conversion efficiencies similar to our best perovskite/silicon tandem with a flat front surface were obtained.

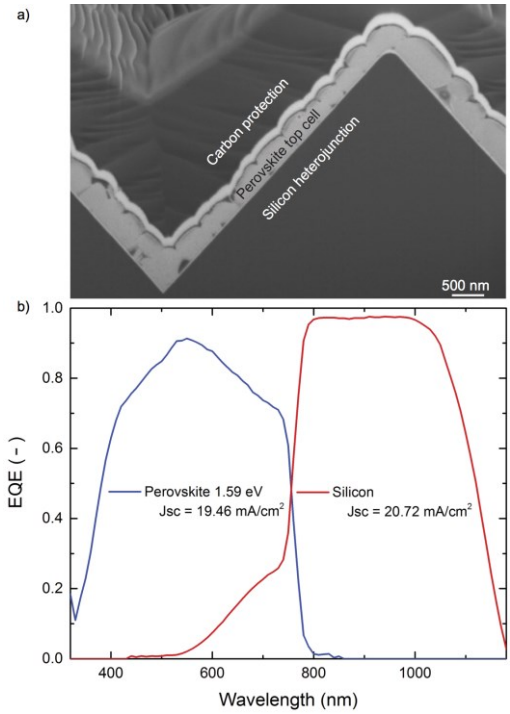


*Figure 4: a) SEM image of the cross-section of a textured tandem prepared using a focused ion beam, b) external quantum efficiency (EQE) of a textured perovskite/silicon monolithic tandem. The perovskite bandgap is 1.59 eV.*

## IV. Conclusion

In this report, we present an hybrid sequential deposition method, where Cs-halides and $PbI_2$ are co-evaporated followed by spin-coating of the organo-halides. This versatile method enables the fabrication of efficient perovskite solar cells with bandgaps between 1.5 and 1.8 eV. More importantly, its allows the conformal deposition of the perovskite layer and its contacts directly on textured silicon wafers. This mitigates reflection losses and paves the way towards a >20 mA/cm$^2$ current-matched monolithic tandem with efficiencies approaching or even surpassing 30%.

## ACKNOWLEDGEMENT

This work was funded by the Nano-Tera.ch Synergy project, the Swiss Federal Office of Energy under Grant SI/501072-01, the Swiss National Science Foundation via the Sinergia Episode (CRSII5_171000) and NRP70 Energy Turnaround PV2050 (407040) projects and from the European Union's Horizon 2020 research and innovation program under Grant Agreements No. 653296 (CHEOPS) and 747221 (POSITS).

## REFERENCES

[1] NREL Efficiency Chart, "NREL Efficiency Chart," 2017.

[2] D. T. Grant, K. R. Catchpole, K. J. Weber, and T. P. White, "Design guidelines for perovskite/silicon 2-terminal tandem solar cells: an optical study," *Opt. Express*, vol. 24, p. 1454, 2016.

[3] J. Werner, B. Niesen, and C. Ballif, "Perovskite/silicon tandem solar cells : marriage of convenience or true love story? – An overview," *Adv. Mater. Interfaces*, vol. 1700731, pp. 1–58, 2017.

[4] K. A. Bush, A. F. Palmstrom, Z. J. Yu, M. Boccard, R. Cheacharoen, J. P. Mailoa, D. P. McMeekin, R. L. Z. Hoye, C. D. Bailie, T. Leijtens, I. M. Peters, M. C. Minichetti, N. Rolston, R. Prasanna, S. Sofia, D. Harwood, W. Ma, F. Moghadam, H. J. Snaith, T. Buonassisi, Z. C. Holman, S. F. Bent, and M. D. McGehee, "23.6%-efficient monolithic perovskite/silicon tandem solar cells with improved stability," *Nat. Energy*, vol. 2, no. 4, p. 17009, Feb. 2017.

[5] F. Sahli, B. A. Kamino, J. Werner, M. Bräuninger, B. Paviet-Salomon, L. Barraud, R. Monnard, J. P. Seif, A. Tomasi, Q. Jeangros, A. Hessler-Wyser, S. De Wolf, M. Despeisse, S. Nicolay, B. Niesen, and C. Ballif, "Improved Optics in Monolithic Perovskite/Silicon Tandem Solar Cells with a Nanocrystalline Silicon Recombination Junction," *Adv. Energy Mater.*, vol. 1701609, p. 1701609, Oct. 2017.

[6] J. Werner, L. Barraud, A. Walter, M. Bräuninger, F. Sahli, D. Sacchetto, N. Tétreault, B. Paviet-Salomon, S.-J. Moon, C. Allebé, M. Despeisse, S. Nicolay, S. De Wolf, B. Niesen, and C. Ballif, "Efficient Near-Infrared-Transparent Perovskite Solar Cells Enabling Direct Comparison of 4‐Terminal and Monolithic Perovskite/Silicon Tandem Cells," *ACS energy Lett.*, vol. 1, p. 474−480, 2016.

[7] T. Duong, Y. L. Wu, H. Shen, J. Peng, X. Fu, D. Jacobs, E. C. Wang, T. C. Kho, K. C. Fong, M. Stocks, E. Franklin, A. Blakers, N. Zin, K. McIntosh, W. Li, Y. B. Cheng, T. P. White, K. Weber, and K. Catchpole, "Rubidium Multication Perovskite with Optimized Bandgap for Perovskite-Silicon Tandem with over 26% Efficiency," *Adv. Energy Mater.*, vol. 7, no. 14, pp. 1–11, 2017.

[8] I. Almansouri, A. Ho-Baillie, S. P. Bremner, and M. A. Green, "Supercharging Silicon Solar Cell Performance by Means of Multijunction Concept," *IEEE J. Photovoltaics*, vol. 5, no. 3, pp. 968–976, 2015.

[9] M. Saliba, T. Matsui, J.-Y. Seo, K. Domanski, J.-P. Correa-Baena, M. K. Nazeeruddin, S. M. Zakeeruddin, W. Tress, A. Abate, A. Hagfeldt, and M. Grätzel, "Cesium-containing triple cation perovskite solar cells: improved stability, reproducibility and high efficiency," *Energy Environ. Sci.*, vol. 9, no. 6, pp. 1989–1997, 2016.

[10] J. Werner, C.-H. Weng, A. Walter, L. Fesquet, J. P. Seif, S. De Wolf, B. Niesen, and C. Ballif, "Efficient Monolithic Perovskite/Silicon Tandem Solar Cell with Cell Area >1 cm 2," *J. Phys. Chem. Lett.*, vol. 7, no. 1, pp. 161–166, Jan. 2016.

[11] E. T. Hoke, D. J. Slotcavage, E. R. Dohner, A. R. Bowring, H. I. Karunadasa, and M. D. McGehee, "Reversible photo-induced trap formation in mixed-halide hybrid perovskites for photovoltaics," *Chem. Sci.*, vol. 6, no. 1, pp. 613–617, 2015.